PLK1 is required for chromosome compaction and microtubule organization in mouse oocytes

Tara M. Little and Philip W. Jordan*
Biochemistry and Molecular Biology Department, Johns Hopkins University Bloomberg School of Public Health, Baltimore, MD 21205

ABSTRACT **Errors during meiotic resumption in oocytes can result in chromosome missegregation and infertility. Several cell cycle kinases have been linked with roles in coordinating events during meiotic resumption, including polo-like kinases (PLKs). Mammals express four kinase-proficient PLKs (PLK1–4). Previous studies assessing the role of PLK1 have relied on RNA knockdown and kinase inhibition approaches, as *Plk1* null mutations are embryonically lethal. To further assess the roles of PLK1 during meiotic resumption, we developed a *Plk1* conditional knockout (cKO) mouse to specifically mutate *Plk1* in oocytes. Despite normal oocyte numbers and follicle maturation, *Plk1* cKO mice were infertile. From analysis of meiotic resumption, *Plk1* cKO oocytes underwent nuclear envelope breakdown with the same timing as control oocytes. However, *Plk1* cKO oocytes failed to form compact bivalent chromosomes, and localization of cohesin and condensin were defective. Furthermore, *Plk1* cKO oocytes either failed to organize α-tubulin or developed an abnormally small bipolar spindle. These abnormalities were attributed to aberrant release of the microtubule organizing center (MTOC) linker protein, C-NAP1, and the failure to recruit MTOC components and liquid-like spindle domain (LISD) factors. Ultimately, these defects result in meiosis I arrest before homologous chromosome segregation.**

Monitoring Editor
Claire Walczak
Indiana University

Received: Dec 24, 2019
Revised: Mar 27, 2020
Accepted: Mar 31, 2020

INTRODUCTION

Meiosis is a specialized cell division that results in the generation of haploid gametes from a diploid precursor germ cell. During meiosis, newly replicated homologous chromosomes become associated with one another via crossover recombination events. During the first meiotic division (meiosis I), homologous chromosomes segregate from one another, whereas sister chromatids remain paired until the second meiotic division (meiosis II). Errors during meiosis can lead to mutation, aneuploidy, and infertility.

Mammalian female meiosis possesses several unique features that are prone to error. First, meiosis is arrested at two different stages. Meiosis is initiated during embryogenesis, and arrests in late prophase, at a stage known as dictyate. During meiotic prophase, before arrest, chromosomes are subjected to induced DNA double-strand breaks that require repair via homologous recombination, which results in at least one crossover recombination event that stably links homologous chromosomes (Gray and Cohen, 2016). The amount of time for this first meiotic arrest differs from one oocyte to another. This is because meiotic prophase arrest is dictated by hormonal induced oocyte maturation, which is cyclical and results in one or a small subset of oocytes maturing for ovulation. It has been well documented that oocytes that remain arrested at dictyate for longer periods of time display depleted levels of proteins that are critical for meiotic resumption and chromosome segregation (Nagaoka *et al.*, 2012; Schatten and Sun, 2015; Webster and Schuh, 2017). For example, the structural maintenance of chromosome (SMC) complexes, cohesin and SMC5/6, have been implicated in increased oocyte age-related errors in chromosome segregation (Jessberger, 2012; MacLennan *et al.*, 2015; Burkhardt *et al.*, 2016; Hwang *et al.*, 2017). Following meiotic resumption, oocytes undergo meiosis I where homologous chromosomes segregate, but sister chromatids remain associated with one another via centromeric cohesion (MacLennan *et al.*, 2015). Sister chromatids then align on a metaphase II plate but remain arrested unless the oocyte is fertilized (Mogessie *et al.*, 2018).

This article was published online ahead of print in MBoC in Press (http://www.molbiolcell.org/cgi/doi/10.1091/mbc.E19-12-0701) on April 8, 2020.

Author contributions: P.W.J. and T.M.L. conceived the project and wrote the manuscript. T.M.L. and P.W.J. performed the experiments.

*Address correspondence to: Philip W. Jordan (pjordan8@jhu.edu).

Abbreviations used: cKO, conditional knockout; GVBD, germinal vesicle breakdown; LISD, liquid-like meiotic spindle domain; MTOC, microtubule organizing center; NEBD, nuclear envelope breakdown; PLK, polo-like kinase.

Another strikingly unique feature of oocytes is that they undergo meiotic divisions in an acentriolar manner. Instead, microtubule organizing centers (MTOCs), containing pericentrosomal components, including CEP192, gamma-tubulin, and NEDD1, are fragmented within the oocyte following nuclear envelope breakdown (NEBD) and the resumption of meiosis I (Ma *et al.*, 2010; Clift and Schuh, 2015; Baumann *et al.*, 2017; Lee *et al.*, 2017; Wang *et al.*, 2017). In parallel to MTOC fragmentation, Aurora A kinase facilitates the distribution of a liquid-like meiotic spindle domain (LISD) by phosphorylating LISD component, TACC3 (So *et al.*, 2019). The LISD is essential for the stabilization of microtubules emanating from the MTOCs. The fragmented MTOCs then coalesce evenly into two MTOC structures on either side of the condensing bivalent chromosomes and form the bipolar spindle required to facilitate chromosome segregation during meiosis I (Namgoong and Kim, 2018). It has been demonstrated that disassociation of C-NAP1, the intercentrosomal linker protein in mitotic cells, from the MTOC must occur before MTOC fragmentation and subsequent downstream steps (Lee and Rhee, 2011; Clift and Schuh, 2015). Inhibition of PLK1 kinase function and depletion of PLK1 via RNA interference (RNAi) have been shown to inhibit C-NAP1 disassociation from MTOCs, which causes defects in MTOC biogenesis and prevents the formation of conventional bipolar spindles (Clift and Schuh, 2015).

To further our collective understanding of the requirements for PLK1 during meiotic resumption in mammals, we utilized a *Plk1* conditional knockout approach to mutate *Plk1* specifically in mouse oocytes before meiotic resumption. We demonstrate the importance of PLK1 in ensuring female fertility and show novel findings with regard to chromosome architecture, and regulation of MTOC and LISD regulation.

RESULTS

Conditional knockout of Plk1 in oocytes results in infertility

We used a floxed *Plk1* allele (*Plk1 flox*) to assess the requirement for PLK1 during meiotic resumption in female mice (Figure 1A; see *Materials and Methods*). Breeding heterozygous *Plk1 flox* mice to mice expressing the Cre recombinase transgene generated a knockout (KO) allele termed *Plk1 del* (Figure 1A). We tested three germ cell–specific Cre transgenes, *Spo11-Cre*, *Gdf9-Cre*, and *Zp3-Cre*. *Spo11-Cre* is expressed during early prophase of meiosis, before the dictyate meiotic arrest (Lyndaker *et al.*, 2013; Hwang *et al.*, 2018b). In contrast, the *Gdf9-Cre* and *Zp3-Cre* are both expressed following the dictyate meiotic arrest, but before resumption of meiosis (Lan *et al.*, 2004). *Gdf9-Cre* is first expressed in primordial follicles by 3 d postpartum (dpp), and *Zp3-Cre* is first expressed in primary follicles by 5 dpp.

We first assessed PLK1 depletion in conditional knockout (cKO) oocytes compared with controls by assessing PLK1 localization via immunofluorescence microscopy during meiotic resumption. Consistent with previous studies (Pahlavan *et al.*, 2000; Xiong *et al.*, 2008; Sun *et al.*, 2012; Clift and Schuh, 2015; Solc *et al.*, 2015; Wang *et al.*, 2017; So *et al.*, 2019), PLK1 localizes to the developing spindle and kinetochores of the condensed bivalents (Figure 1, B and D). Surprisingly, despite observing efficient deletion of the floxed third exon of *Plk1* (Supplemental Figure S1A), cKO of *Plk1* using *Gdf9-Cre* or *Zp3-Cre* did not result in depletion of PLK1 protein (Supplemental Figure S1, B and C). These observations demonstrate that mRNA levels and protein levels before conditional mutation of the *Plk1 flox* allele are sufficient to maintain PLK1 protein levels during meiotic progression. In contrast, using the *Spo11-Cre* transgene resulted in the absence of PLK1 protein in *Plk1* cKO oocytes in metaphase I (Figure 1, C and E and Supplemental Figure S1, D and E). Therefore, we focused on *Plk1*, *Spo11-Cre* cKO mice in this study.

Breeding *Plk1 +/flox, Spo11-Cre* females to wild-type males showed that mutation of the *Plk1 flox* allele mediated by *Spo11-Cre* was 90% efficient (Supplemental Figure S1A). Because *Spo11-Cre* is expressed in early prophase, it is possible that defects could be occurring in newborn oocytes, before the dictyate arrest. Therefore, we assessed the meiotic stages of oocytes from newborn females and did not observe morphological differences with regard to prophase stage distribution, or synapsis and desynapsis morphology (Figure 1, F and G).

Plk1 cKO oocytes fail to form polar bodies

Adult *Plk1, Spo11-Cre* cKO females failed to produce litters ($N = 5$). Despite this infertility, *Plk1* cKO females had normal ovarian morphology and equivalent oocyte numbers (Figure 2, A and B). We isolated oocytes from control and *Plk1*, *Spo11-Cre* cKO mice and assessed synchronized meiotic resumption in vitro. We measured nuclear envelope breakdown (NEBD, also known as germinal vesicle breakdown, GVBD) and first polar body formation. NEBD was equivalent between controls and *Plk1*, *Spo11-Cre* cKO oocytes (Figure 2C). To address whether oocytes would reach a metaphase II arrest stage, we assessed ovulated oocytes harvested from the ampulla. At this timepoint, control oocytes were arrested in metaphase II with an attached polar body. In contrast, *Plk1*, *Spo11-Cre* cKO failed to extrude the first polar body (Figure 2D). Assessment of oocytes via immunofluorescence microscopy indicated that *Plk1*, *Spo11-Cre* cKO oocytes failed to undergo metaphase-to-anaphase transition during meiosis I (Figure 2E). Thus, our studies focused on the transition from NEBD to metaphase I.

Plk1 cKO oocytes show abnormal chromosome compaction

During meiotic resumption, homologous chromosomes associated via chiasmata (crossovers) condense and form easily discernible bivalent structures (Figure 3A). We assessed bivalent formation, and compared axis morphology between the control and *Plk1*, *Spo11-Cre* cKO by analyzing cohesin and condensin localization in oocytes 6 h after meiotic resumption. From observing chromosome spread preparations, almost all control oocytes display bivalent chromosome morphology (Figure 3, A and B). In contrast, 40% of *Plk1*, *Spo11-Cre* cKO oocytes failed to form compact chromosomes, instead having dispersed chromatin signal where resolution between separate chromosome pairs was not evident. We assessed axis formation in more detail by analyzing REC8 and SMC4, cohesin and condensin components, respectively. REC8-cohesin complexes form a single axial structure along the bivalent core (Figure 3C). The expected axial localization of cohesin was observed for most chromatin spread preparations of control oocytes (Figure 3, C and D). However, 40% of *Plk1*, *Spo11-Cre* cKO oocytes displayed only partial cohesin axis formation. Condensin forms two separate axes within the bivalent (Figure 3E). The chromatin morphology defects observed for *Plk1*, *Spo11-Cre* cKO were further highlighted by assessing condensin localization where the majority of oocytes had only partial condensin axial localization (55%), and a significant number with dispersed condensin localization throughout the chromatin (24%; Figure 3, E and F).

Plk1 cKO oocytes fail to form normal bipolar metaphase I spindles

During meiotic resumption, acentriolar MTOC components fragment throughout the oocyte, then coalescence evenly on either side of the condensing bivalents to form the bipolar metaphase I spindle

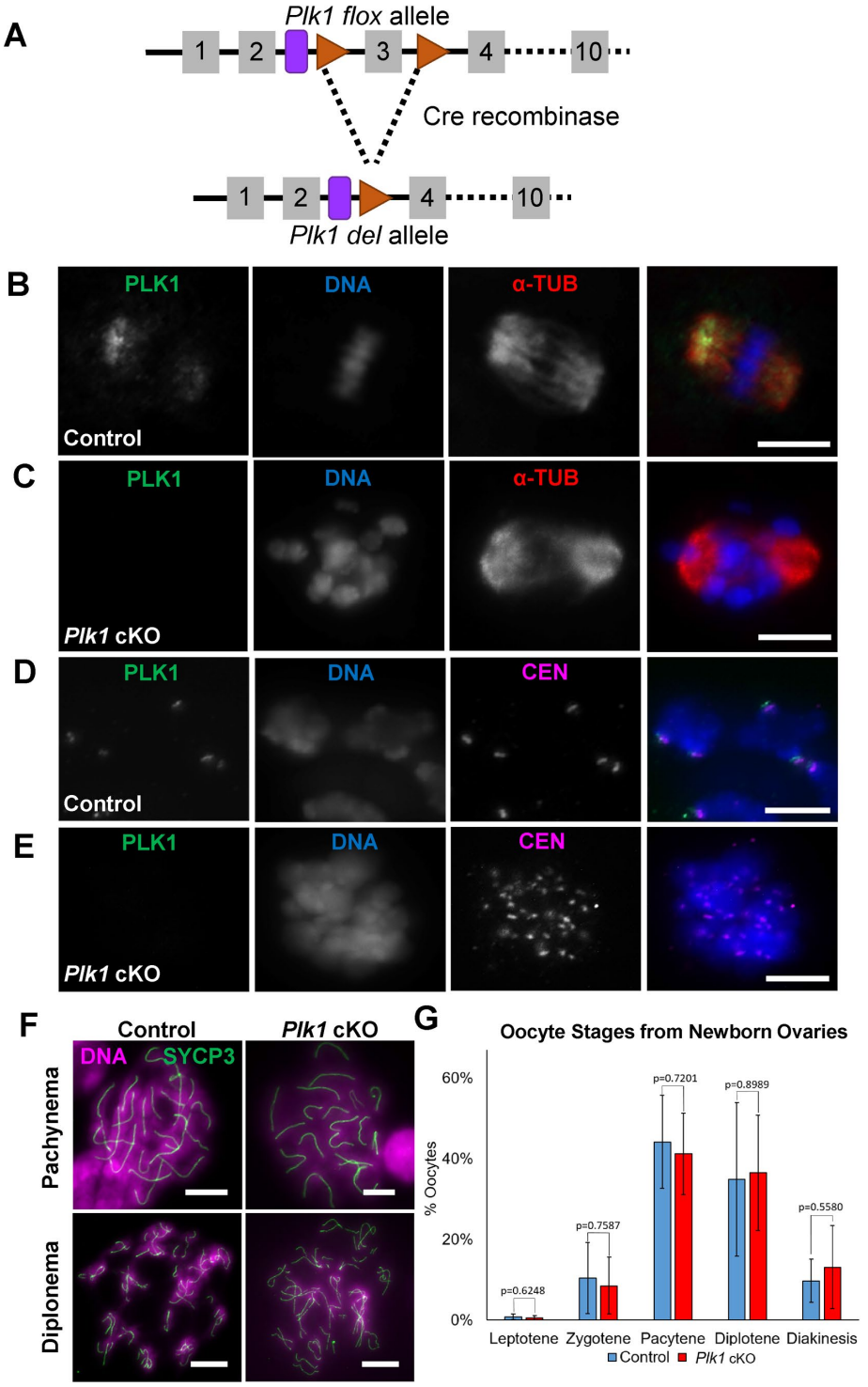

FIGURE 1: PLK1 localizes to the microtubule organizing centers and centromeres in oocytes. (A) Schematic of mouse *Plk1* floxed allele containing loxP sites (red triangle), flanking exon 4 (gray box), and the resulting *Plk1* deletion allele after excision of exon 3 by Cre recombinase in early prophase. The purple round-sided rectangle represents the remaining Frt site following FLP-mediated recombination of the original conditional ready tm1a allele (see *Materials and Methods*). (B, C) Control (B) and *Plk1* cKO (C) oocytes immunolabeled with antibodies against PLK1 (green) and alpha-tubulin (α-TUB, red), and counterstained with DAPI (DNA, blue). Scale bar: 10 μm. (D, E) Chromatin spread preparation of control (D, scale bar: 5 μm) and *Plk1* cKO (E, scale bar: 5 μm) oocytes immunolabeled with antibodies against PLK1 (green) and centromeres/kinetochores (CEN, purple), and counterstained with DAPI (DNA, blue). (F) Chromatin spread preparations of control and *Plk1* cKO pachytene- and diplotene-stage oocytes harvested from newborn females (2 dpp). Spreads are stained with SYCP3 (green) and counterstained with DAPI (DNA, purple). Scale bar: 10 μm. (G) Quantification of meiosis I stages of oocytes harvested from newborn females (1–2 dpp). Six control mice and four *Plk1* cKO mice were assessed, with 100 oocytes counted per mouse. Mean and SD of each column are represented by the black bars. No significant difference between the control and *Plk1* cKO was observed according to a Mann-Whitney test (two-tailed).

required to mediate chromosome segregation during meiosis I (Clift and Schuh, 2015). We first assessed bipolar spindle formation, using antibodies raised against alpha-tubulin, 6 h after meiotic resumption. From observing whole-oocyte preparations, almost all control oocytes developed a bipolar metaphase I spindle (Figure 4, A and B). In contrast, 60% of *Plk1*, *Spo11-Cre* cKO oocytes formed a bipolar spindle, and the remaining 40% of oocytes did not harbor any alpha-tubulin signal. From further analyses of the bipolar spindle that formed in 60% of *Plk1*, *Spo11-Cre* cKO oocytes, we determined that the alpha-tubulin spindle length and width were reduced compared with the control oocytes (Figure 4, C–E). Taken together, these data indicate that PLK1 is important for regulation of acentriolar MTOC dynamics following meiotic resumption in mouse oocytes, which is critical for the formation of bipolar spindles that are capable of mediating chromosome segregation during the metaphase-to-anaphase I transition.

Plk1 cKO oocytes display defects in MTOC and LISD distribution

Although we did observe bipolar spindles in 60% of the *Plk1*, *Spo11-Cre* cKO oocytes, these were morphologically abnormal, being both shorter in length and width (Figure 4). Therefore, we hypothesized that the regulation of acentriolar MTOCs may be perturbed in *Plk1*, *Spo11-Cre* cKO oocytes. We first assessed the localization of the centrosomal linker protein, C-NAP1. Before NEBD, C-NAP1 localizes as a dense focus at unfragmented acentriolar MTOCs in control and *Plk1*, *Spo11-Cre* cKO oocytes (Figure 5, A and B). In control oocytes, C-NAP1 signal diminishes during prometaphase, and alpha-tubulin spindles begin to elongate and eventually form a bipolar spindle at metaphase I (Figure 5A). In contrast, C-NAP1 remains as a dense focus in *Plk1*, *Spo11-Cre* cKO oocytes at prometaphase (Figure 5, B and C). Notably, the prometaphase spindle in *Plk1* cKO oocytes appears smaller than those in control

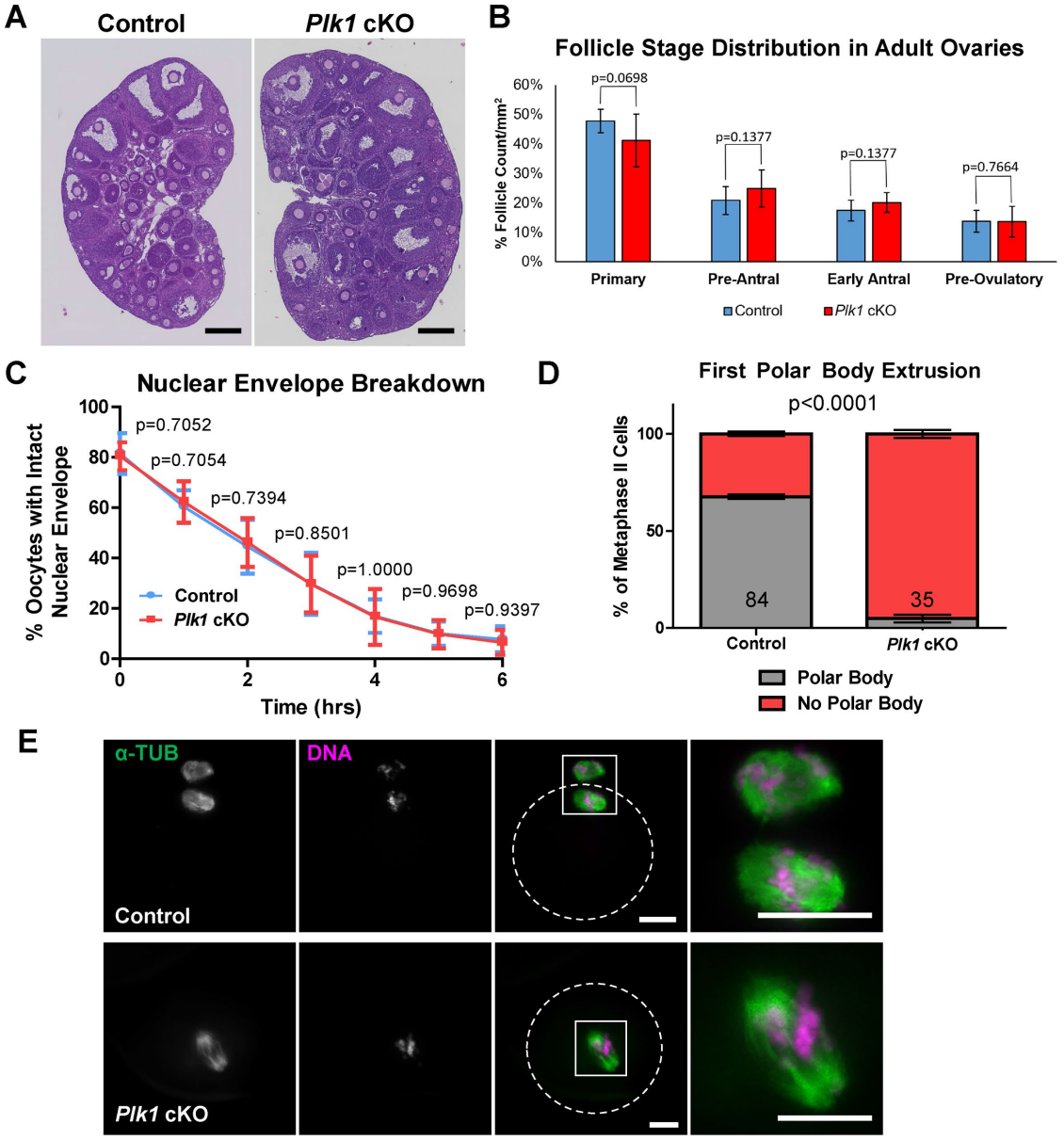

FIGURE 2: *Plk1* cKO follicle numbers and NEBD timing are equivalent to control, but oocytes fail to extrude the first polar body. (A) Cross sections of ovaries from adult control and *Plk1* cKO mice stained with hematoxylin and eosin. Scale bar: 250 μm. (B) Quantification of follicle stages from hematoxylin and eosin stained ovaries from control and *Plk1* cKO mice. Ten ovaries were counted per genotype. Mean and SD of the columns of each graph are represented by the black bars. No significant difference between the control and *Plk1* cKO was observed according to a Mann-Whitney test (two-tailed). (C) Timing of NEBD in oocytes from control and *Plk1* cKO mice. Oocytes (434) from 10 control mice and 401 oocytes from 10 *Plk1* cKO mice were assessed. Mean and SD of the columns of each graph are represented by the blue circles (control), pink squares (*Plk1* cKO), and corresponding bars. No significant difference between the control and *Plk1* cKO was observed according to a Mann-Whitney test (two-tailed). (D) Quantification of first polar body extrusion in control and *Plk1* cKO metaphase II oocytes collected from ampullas. Oocytes (84) from 5 control mice and 35 oocytes from 4 *Plk1* cKO mice were assessed. The majority of control oocytes scored without a polar body are likely a result of polar body loss during the collection and staining process. Bars represent 95% confidence intervals, and the *P* value (Mann-Whitney, two-tailed) for the indicated comparison is significant ($P < 0.0001$). (E) Examples of metaphase II control and *Plk1* cKO oocytes stained for alpha-tubulin (α-TUB, green) and DNA (DAPI, purple). Dotted circles indicate the outline of oocytes. Scale bar: 20 μm.

oocytes. This implies that the defects resulting in smaller metaphase spindles are already occurring in prometaphase.

Fragmentation of MTOCs following meiotic resumption in oocytes requires the dissociation of C-NAP1, during NEBD (Lee and Rhee, 2011; Clift and Schuh, 2015). Therefore, we hypothesized that the aberrancies in C-NAP1 dispersal following NEBD (Figure 5) likely affects MTOC component localization in *Plk1*, *Spo11-Cre* cKO oocytes. We first assessed gamma-tubulin localization, which is a component of acentriolar MTOCs and spindle microtubules (Figure 6, A and B; So *et al.*, 2019). Interestingly, the 44% of *Plk1*, *Spo11-Cre*

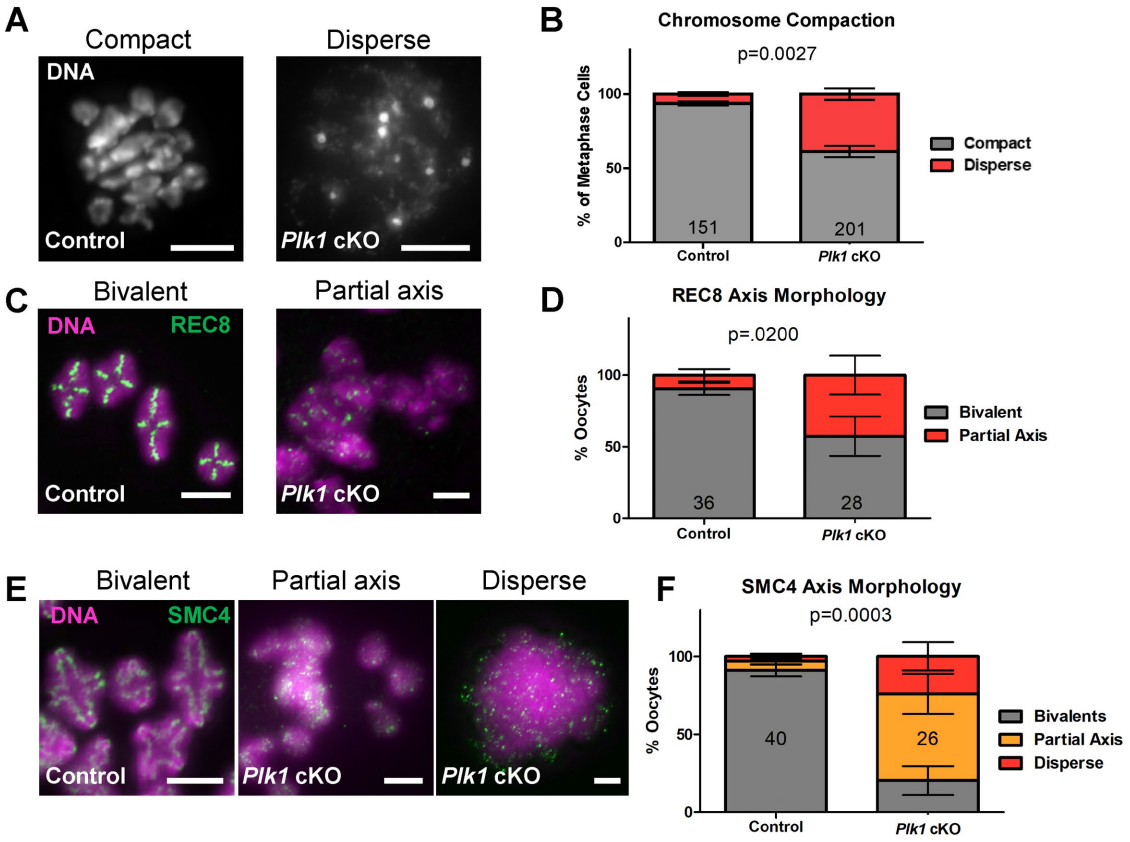

FIGURE 3: *Plk1* cKO oocytes undergo abnormal chromosome compaction following NEBD. (A) Chromatin spread preparation of control (on the left, compact) and *Plk1* cKO (on the right, disperse) oocytes counterstained with DAPI (DNA). Scale bar: 10 µm. (B) Quantification of chromatin compaction. 151 oocytes from 19 control mice and 201 oocytes from 14 *Plk1* cKO mice were assessed. Bars represent 95% confidence intervals, and the *P* value (Mann-Whitney test, two-tailed) for the indicated comparison is significant ($P = 0.0027$). (C) Chromatin spreads of control and *Plk1* cKO oocytes immunolabeled with antibodies against REC8 (green), and counterstained with DAPI (DNA, purple). Scale bar: 5 µm. (D) Quantification of REC8 axis morphology. Oocytes (36) from 11 control mice and 28 oocytes from 9 *Plk1* cKO mice were assessed. Bars represent 95% confidence intervals, and the *P* value (Mann-Whitney test, two-tailed) for the indicated comparison is significant ($P = 0.02$). (E) Chromatin spreads of control and *Plk1* cKO oocytes immunolabeled with antibodies against SMC4 (green), and counterstained with DAPI (DNA, purple). Scale bar: 2 µm. (F) Quantification of SMC4 axis morphology. Oocytes (40) from 10 control mice and 26 oocytes from 9 *Plk1* cKO mice were assessed. Bars represent 95% confidence intervals, and the *P* value (Mann-Whitney test, two-tailed) for the indicated comparison is significant ($P = 0.0003$).

cKO oocytes that had bipolar alpha-tubulin spindles lacked gamma-tubulin signals. In addition, 37% of *Plk1*, *Spo11-Cre* cKO oocytes had monopolar gamma-tubulin signals often with little or no alpha-tubulin signal. In contrast, 81% of control oocytes had bipolar gamma-tubulin signals.

We then assessed the localization of two components of acentriolar MTOCs, CEP192 and NEDD1, in oocytes with bipolar alpha-tubulin spindles. In control oocytes, CEP192 and NEDD1 distribute evenly at both alpha-tubulin spindle poles (Figure 6, C–F). A CEP192 signal was absent in the majority (70%) of *Plk1*, *Spo11-Cre* cKO oocytes (Figure 6, C and D). Similar results were obtained for NEDD1 with 74% of *Plk1*, *Spo11-Cre* cKO oocytes not harboring a NEDD1 signal (Figure 6, E and F). These oocytes also had unorganized chromosomes, further supporting a chromosome compaction defect.

The MTOC assembly process is temporally coordinated with the organization of the LISD. Aurora A regulates the distribution of the LISD by phosphorylating TACC3, a critical LISD component (So *et al.*, 2019). While Aurora A localized to the alpha-tubulin spindle poles in control metaphase I oocytes, Aurora A was absent in most (78%) of the *Plk1* cKO oocytes (Figure 7, A and B). In control oocytes, TACC3 localizes to the bipolar spindle (Figure 7, C and D). However, the majority (78%) of *Plk1*, *Spo11-Cre* cKO oocytes did not have a TACC3 signal localized to any portion of the spindle.

DISCUSSION

PLK1 and NEBD

PLKs have been associated with many stages of the cell cycle, including NEBD. Disassembly of nuclear pore complexes (NPCs) is known to be a key aspect of NEBD, required for nuclear envelope permeabilization (Champion *et al.*, 2017). PLK-1 in *Caenorhabditis elegans* and PLK1 in human cells has been shown to localize to the nuclear periphery, colocalizing with NPCs during late prophase. Mutation of PLK-1 or kinase inhibition of mammalian PLK1 results in aberrant NEBD because PLK1 is required for phosphorylation of components of the NPC, which subsequently results in NPC disassembly (Linder *et al.*, 2017; Martino *et al.*, 2017; de Castro *et al.*, 2018).

NEBD is the first stage of meiotic resumption in oocytes. In a previous report, PLK1 kinase inhibition in mouse oocytes was shown

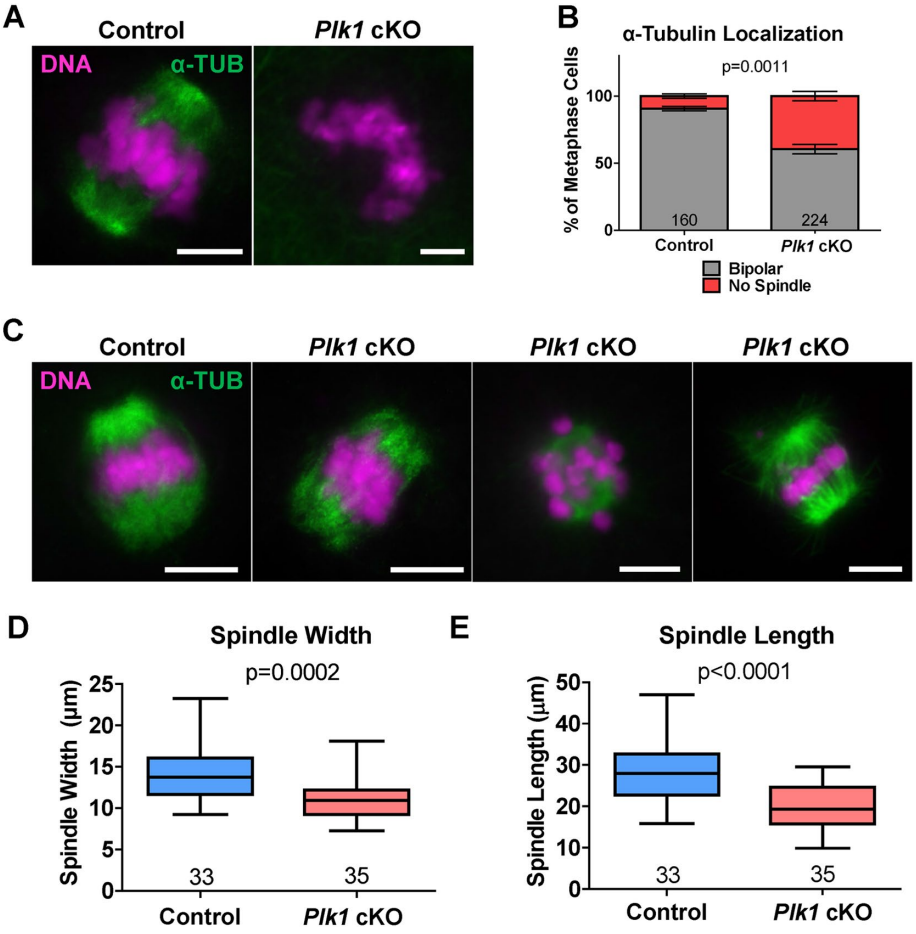

FIGURE 4: *Plk1* cKO oocytes form abnormal alpha-tubulin spindle structures during meiotic resumption. (A) Examples of control and *Plk1* cKO oocytes immunolabeled with antibodies against alpha-tubulin (α-TUB, green), and counterstained with DAPI (DNA, purple). Scale bar: 10 μm. (B) Quantification of alpha-tubulin localization. Oocytes (160) from 18 control mice and 224 oocytes from 14 *Plk1* cKO mice were assessed. Bars represent 95% confidence intervals, and the *P* value (Mann-Whitney test, two-tailed) for the indicated comparison is significant ($P = 0.0011$). (C) Examples of an average sized control spindle and small *Plk1* cKO spindles immunolabeled with antibodies against alpha-tubulin (α-TUB, green), and counterstained with DAPI (DNA, purple). Scale bar: 10 μm. (D) Box plot of spindle length from each spindle pole. Oocytes (33) from 9 control mice and 35 oocytes from 8 *Plk1* cKO mice were assessed. Whiskers represent minimum and maximum values, and the *P* value (Mann-Whitney test, two-tailed) for the indicated comparison is significant ($P < 0.0001$). (E) Box plot of the width of each spindle pole. Oocytes (33) from 9 control mice and 35 oocytes from 8 *Plk1* cKO mice were assessed. Whiskers represent minimum and maximum values, and the *P* value (Mann-Whitney test, two-tailed) for the indicated comparison is significant ($P = 0.0002$).

to delay meiotic resumption with regard to NEBD (Solc *et al.*, 2015). Our results contrast this observation as NEBD was equivalent between controls and *Plk1*, *Spo11-Cre* cKO oocytes. However, the delay in NEBD caused by PLK1 kinase inhibition is small when comparing to CDK1 inhibition (Solc *et al.*, 2015). PLK1 is known to be involved in activation of CDK1 (Jackman *et al.*, 2003), but may not be essential for its role in NEBD in oocytes. Taken together, the NEBD role of PLK1 in mammalian oocytes is likely minor and does not result in the arrest of meiotic resumption.

Role for PLK1 during chromosome compaction before segregation

PLK1 has been shown to interact with and phosphorylate components of condensin in cultured human cancer cell lines, and these processes are important to facilitate proficient chromosome condensation and chromosome segregation (Abe *et al.*, 2011; Kim *et al.*, 2014). In addition, PLK1 contributes to cohesin release during G2-phase in mitotically dividing cells, which is important for normal chromosome compaction (Haarhuis *et al.*, 2014). In budding yeast, it has been shown that the sole PLK homologue, Cdc5, is required for cohesin release, which coincides with PLK-dependent compaction of chromosomes before their segregation during meiosis I (Lee and Amon, 2003; Attner *et al.*, 2013; Challa *et al.*, 2019).

In mouse oocytes, PLK1 has been shown to accumulate at kinetochores, but there is also a PLK1 signal detected along bivalent chromosomes (Solc *et al.*, 2015). Here, we demonstrate *Plk1* cKO causes chromosomes to compact abnormally following NEBD, with cohesin and condensin axis formation defects. RNAi-mediated depletion or kinase inhibition of PLK1 resulted in delayed chromosome individualization after NEBD, with chromosomes remaining clumped together (Clift and Schuh, 2015). It was suggested that these observations were due to the MTOC fragmentation defects. However, based on previous studies linking PLK1 with chromatin dynamics, it is possible that PLK1 plays a direct role in the formation of individual bivalents in oocytes.

PLK1 is essential for acentriolar bipolar spindle formation in oocytes

Mammalian oocytes do not harbor centrioles, and instead rely on multiple acentriolar MTOCs that fragment from one another following NEBD, then subsequently coalesce evenly on each side of the condensed bivalents and form bipolar spindles (Clift and Schuh, 2015). Similar to work assessing the role of PLK1 in oocytes using siRNA and kinase inhibition approaches, we demonstrated that PLK1 is required for spindle integrity to ensure the formation of normal bipolar spindles capable of facilitating chromosome segregation during meiosis I (Clift and Schuh, 2015; Solc *et al.*, 2015; Liao *et al.*, 2018). Furthermore, using the *Plk1* cKO strategy, we complemented previous RNAi and kinase inhibitor approaches that showed that PLK1 is required for C-NAP1 dissociation during NEBD, which is critical for fragmentation of MTOC components (Clift and Schuh, 2015). In mitosis, both C-NAP1 dissociation and centrosome separation are initiated by PLK1 (Mardin *et al.*, 2011), demonstrating that although oocytes are acentriolar the importance of PLK1 in bipolar spindle formation is universal.

We showed that PLK1 is required for normal localization of acentriolar MTOC components gamma-tubulin, CEP192, and NEDD1. We observed a complete absence of gamma-tubulin at MTOCs in the majority of *Plk1* cKO oocytes, which is consistent with the observations made when PLK1 kinase activity was inhibited (Solc *et al.*, 2015). With regard to CEP192, we mostly observe a complete

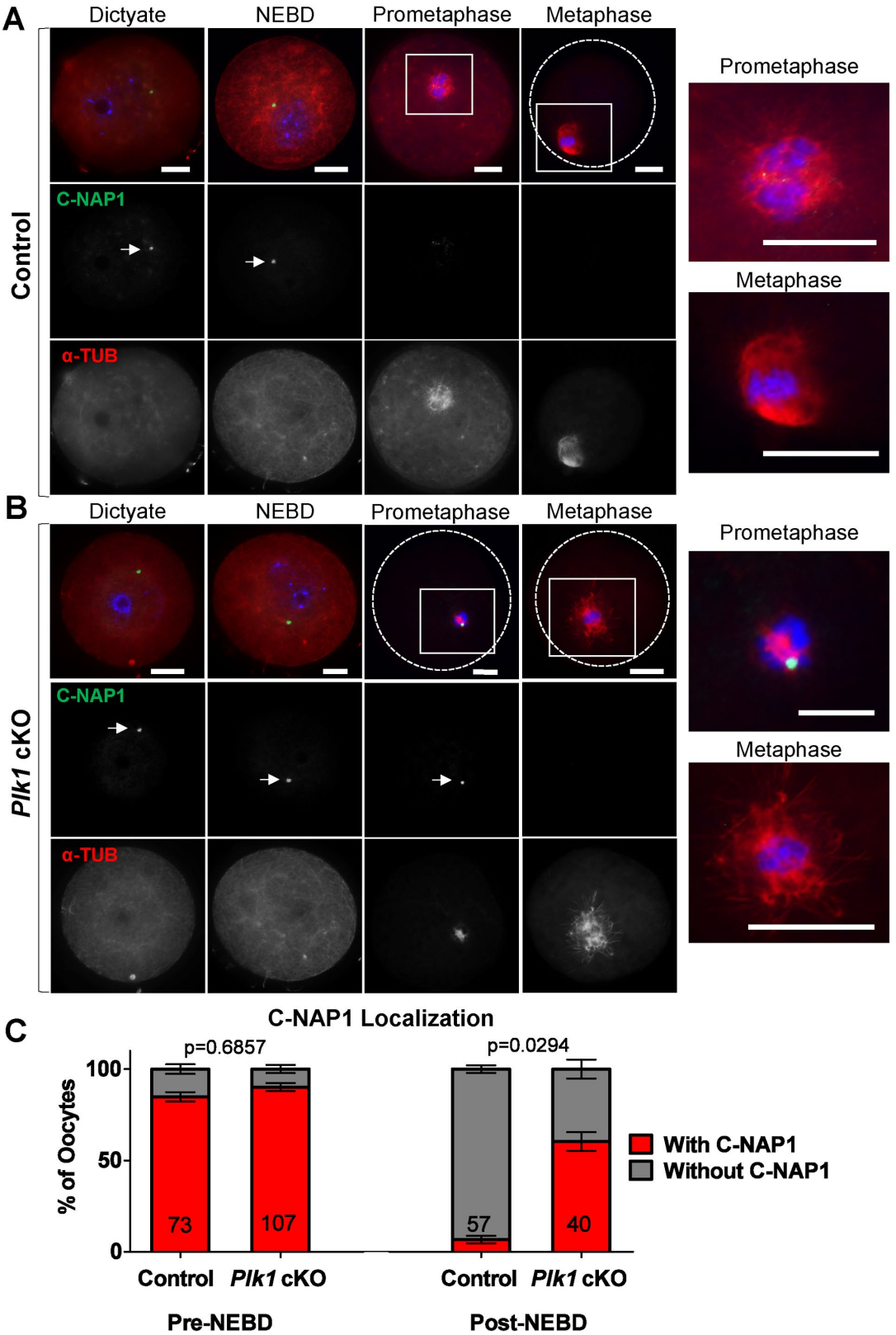

FIGURE 5: *Plk1* cKO oocytes fail to disperse C-NAP1 following meiotic resumption. (A, B) Control (A) and *Plk1* cKO (B) oocytes immunolabeled with antibodies against C-NAP1 (green) and alpha-tubulin (α-TUB, red), and counterstained with DAPI (DNA, blue). Solid squares indicate the source of zoomed images on the right. Dotted circles indicate the oocyte outline. Meiotic stages were determined based on alpha-tubulin and DAPI staining. Scale bar: 20 μm. (C) Quantification of C-NAP1 localization in pre-NEBD control ($n = 73$) and *Plk1* cKO ($n = 107$) oocytes, and post-NEBD control ($n = 57$) and *Plk1* cKO ($n = 40$) oocytes. Bars represent 95% confidence intervals, and the *P* value (Mann-Whitney test, two-tailed) for pre-NEBD was not significant ($P = 0.6857$), and for post-NEBD is significant ($P = 0.0294$).

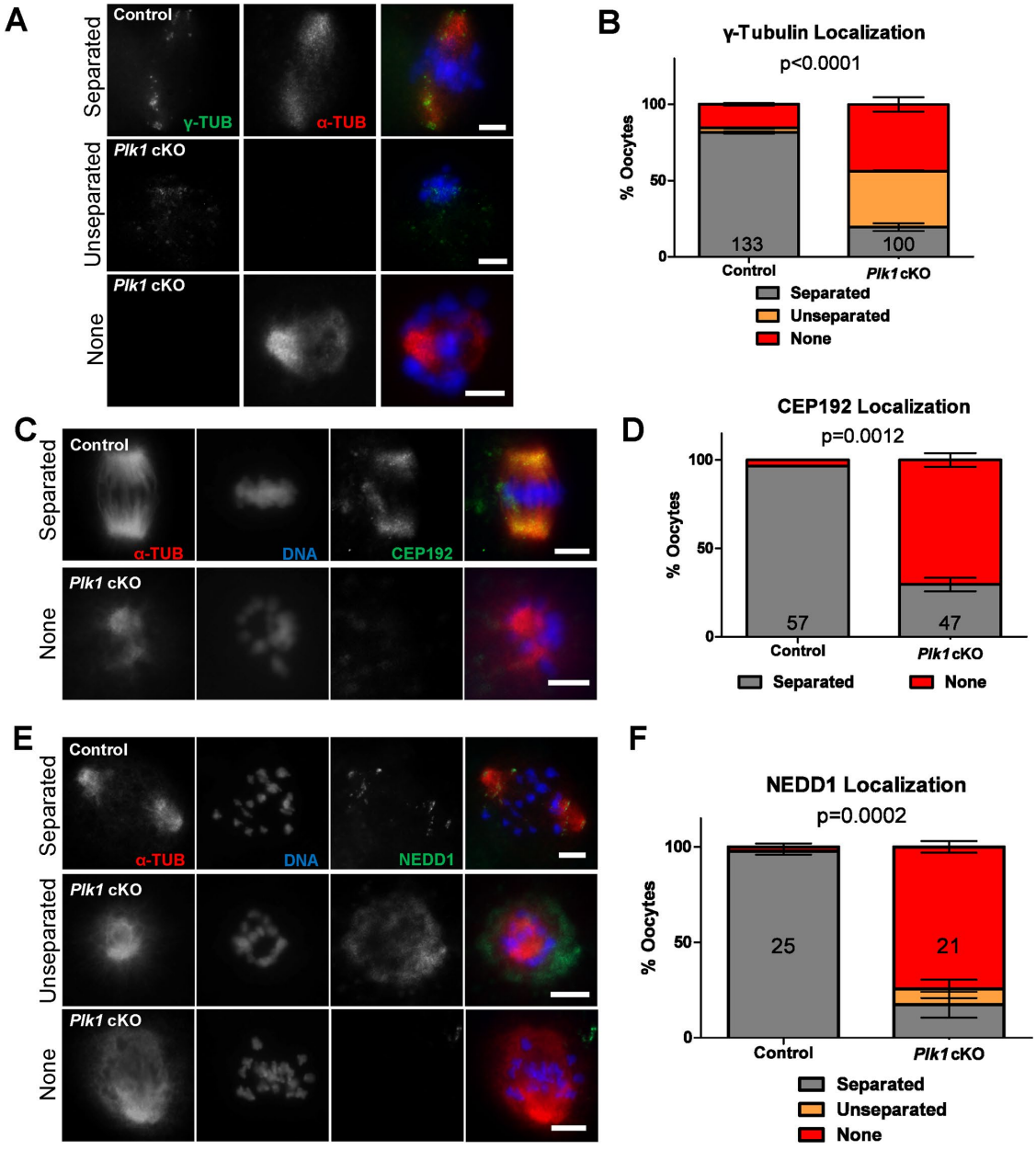

FIGURE 6: *Plk1* cKO oocytes display abnormal localization of MTOC components. (A) Examples of control and *Plk1* cKO metaphase I oocytes immunolabeled with antibodies against gamma-tubulin (γ-TUB, green) and alpha-tubulin (α-TUB, red), and counterstained with DAPI (DNA, blue). Scale bar: 10 μm. (B) Quantification of gamma-tubulin localization in metaphase I oocytes. Oocytes (133) from 3 control mice and 100 oocytes from 3 *Plk1* cKO mice were assessed. Bars represent 95% confidence intervals, and the *P* value (Mann-Whitney test, two-tailed) for the indicated comparison is significant ($P < 0.0001$). (C) Examples of control and *Plk1* cKO oocytes immunolabeled with antibodies against MTOC component, CEP192 (green), and alpha-tubulin (α-TUB, red), and counterstained with DAPI (DNA, blue). (D) Quantification of CEP192 localization. Oocytes (57) from 3 control mice and 47 oocytes from 3 *Plk1* cKO mice were assessed. Bars represent SD, and the *P* value (Mann-Whitney test, two-tailed) for the indicated comparison is significant ($P = 0.0012$). (E) Examples of control and *Plk1* cKO oocytes immunolabeled with antibodies against MTOC component, NEDD1 (green), and alpha-tubulin (α-TUB, red), and counterstained with DAPI (DNA, blue). (F) Quantification of NEDD1 localization. Oocytes (25) from 5 control mice and 21 oocytes from 5 *Plk1* cKO mice were assessed. Bars represent 95% confidence intervals, and the *P* value (Mann-Whitney test, two-tailed) for the indicated comparison is significant ($P = 0.002$).

absence of the protein to MTOCs, whereas PLK1 inhibition led to monopolar localization of CEP192 (Clift and Schuh, 2015). The effects of PLK1 functional loss on NEDD1 had not previously been assessed in oocytes. However, in human cell lines PLK1 phosphorylates NEDD1 and increases its anchoring capacity for gamma-tubulin onto centrosomes (Zhang *et al.*, 2009). The formation of an abnormally small spindle in *Plk1* cKO oocytes may be due to an alternative microtubule assembly pathway. Prior studies have shown that kinetochore-dependent microtubule assembly may compensate for the loss of canonical centrosomes in mammalian cells

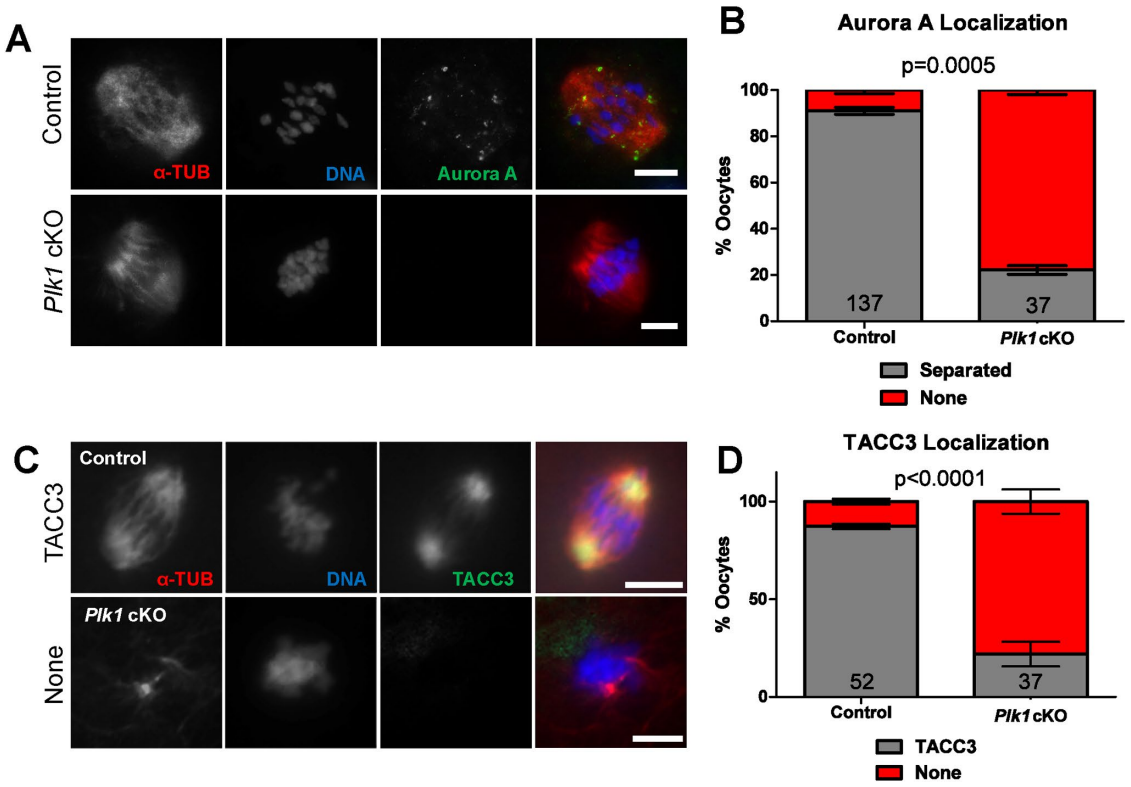

FIGURE 7: *Plk1* oocytes display abnormal localization of LISD components. (A) Examples of control and *Plk1* cKO metaphase I oocytes immunolabeled with antibodies against alpha-tubulin (α-TUB, red) and Aurora A (green), and counterstained with DAPI (DNA, blue). Scale bar: 10 μm. (B) Quantification of Aurora A localization in metaphase I oocytes. Oocytes (137) from 2 control mice and 37 oocytes from 3 *Plk1* cKO mice were assessed. Bars represent 95% confidence intervals, and the *P* value (Mann-Whitney test, two-tailed) for the indicated comparison is significant ($P = 0.0005$). (C) Examples of control and *Plk1* cKO oocytes immunolabeled with antibodies against LISD component, TACC3 (green), and alpha-tubulin (α-TUB, red), and counterstained with DAPI (DNA, blue). (D) Quantification of TACC3 localization. Oocytes (52) from 3 control mice and 37 oocytes from 3 *Plk1* cKO mice were assessed. Bars represent 95% confidence intervals, and the *P* value (Mann-Whitney test, two-tailed) for the indicated comparison is significant ($P < 0.0001$). Scale bars: 10 μm.

(Mishra *et al.*, 2010; Prosser and Pelletier, 2017). It is possible that such a pathway explains the presence of alpha-tubulin in oocytes without gamma-tubulin, as observed in our work and others (Solc *et al.*, 2015). Research in mammalian mitotic cells has demonstrated that microtubules can be nucleated and emanated from kinetochores when PLK1 is depleted (Torosantucci *et al.*, 2008). These kinetochore-based microtubules, driven by the RanGTP gradient, can organize themselves into spindle poles. This may explain the unstable bipolar spindles observed in *Plk1* cKO oocytes.

A recent, comprehensive study of factors required for bipolar spindle formation in oocytes discovered that TACC3 is a major component of a novel LISD (So *et al.*, 2019). The same study presented that Aurora A kinase, but not PLK1 kinase activity, is required for LISD maintenance. These experiments were designed to inhibit PLK1 and Aurora A at metaphase I stage oocytes, which is different from our experimental design using *Plk1* cKO oocytes. Our results indicate that PLK1 does indeed play a role in LISD maintenance upstream of Aurora A. This is further supported by the observation that Aurora A and TACC3 are not recruited to the spindle in *Plk1* cKO oocytes. In support of our observations, a study using human cell lines determined that PLK1 inhibition resulted in down-regulation of TACC3 targeting to mitotic spindles (Fu *et al.*, 2013). Taken together, our results show that PLK1 activity is required for C-NAP1 dissociation, normal acentriolar MTOC fragmentation, and localization of MTOC and LISD components that are important to ensure formation of a bipolar spindle (Figure 8). These processes are critical for an oocyte to progress through meiosis I and be capable of fertilization, demonstrating that PLK1 is essential for female fertility in mammals.

MATERIALS AND METHODS

Ethics statement

All mice were bred at Johns Hopkins University (JHU, Baltimore, MD) in accordance with the National Institutes of Health and U.S. Department of Agriculture criteria. Protocols for their care and use were approved by the Institutional Animal Care and Use Committees of JHU.

Mice

mESC clones HEPD0663_7_E04 (C57BL/6N-A/a genetic background) bearing a "knockout first" allele of *Plk1* (*Plk1*tm1a(EUCOMM)Hmgu) were acquired from the Knockout Mouse Project (https://www.mousephenotype.org/data/genes/MGI:97621).

Chimeras were obtained by microinjection of HEPD0663_7_E04 mESCs into C57BL/6JN blastocyst-stage mouse embryos and assessed for germline transmission. Heterozygous progeny were bred with a C57BL/6J Flp recombinase deleter strain (B6.129S4-*Gt(ROSA)26Sor*tm1(FLP1)Dym/RainJ, JAX) to remove the *SA-LacZ*

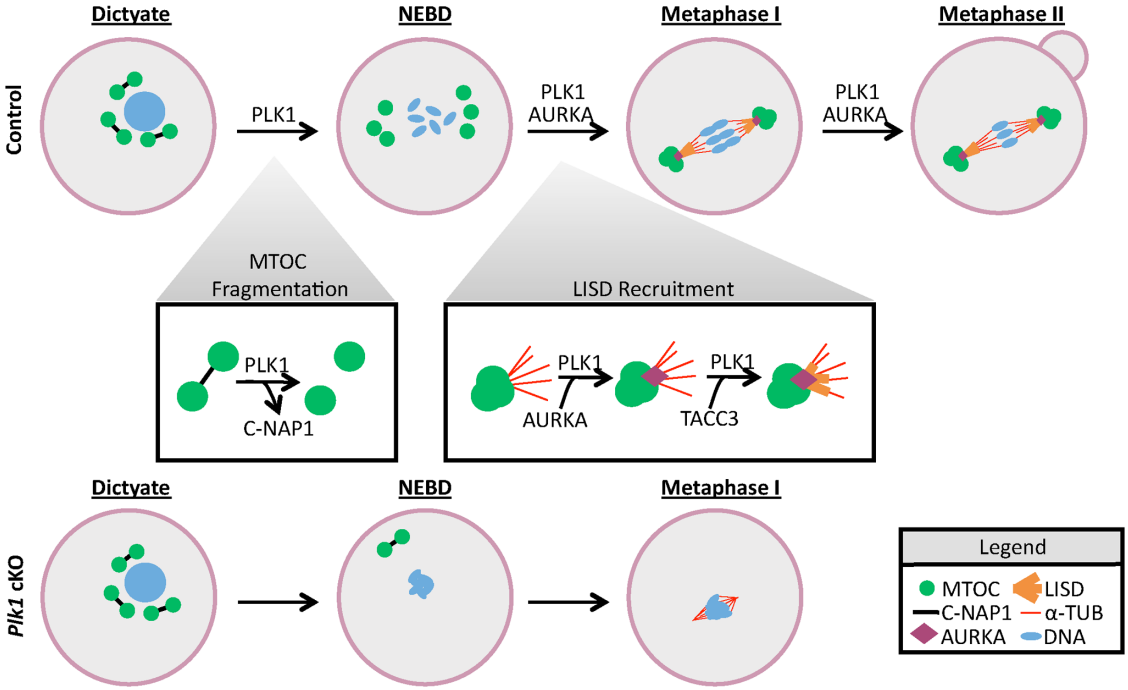

FIGURE 8: PLK1 regulates chromosome condensation, MTOC fragmentation, and LISD recruitment in mammalian oocytes. In control oocytes, PLK1 is responsible for dissociating C-NAP1 immediately after meiotic resumption. This allows MTOC components to fragment and then coalesce evenly on both sides of the condensed bivalents and form bipolar spindles. As oocytes enter metaphase, PLK1 is required for the recruitment of Aurora A (AURKA) to the MTOC and bipolar spindle. Aurora A then recruits TACC3, the major component of the LISD. In *Plk1* cKO oocytes, chromosomes do not properly condense following meiotic resumption. Furthermore, C-NAP1 is not dissociated in an efficient manner in *Plk1* cKO oocytes. This leads to MTOC (γ-tubulin, CEP192, and NEDD1) and LISD (Aurora A and TACC3) components failing to localize and cluster, and results in MTOC failure and abnormal spindle formation. Microtubules that do polymerize in *Plk1* cKO oocytes form a small, abnormal metaphase spindle, which is likely driven by a kinetochore-dependent microtubule assembly pathway (Torosantucci *et al.*, 2008; Prosser and Pelletier, 2017). Ultimately, the defects observed in *Plk1* cKO oocytes lead to arrest in metaphase I.

and *Neo* selection cassette and produce the floxed exon 4 (designated *Plk1 flox*).

To produce offspring heterozygous for the deleted exon 4 (designated *Plk1 del*), heterozygous *Plk1 flox* males were mated to *Sox2-Cre* C57BL/6J (B6.Cg-Tg(Sox2-cre)1Amc/J, JAX) mice.

Further, heterozygous *Plk1 del* mice were bred to mice harboring the Cre transgenes that are specifically expressed in germ cells—*Spo11-Cre* (C57BL/6-Tg Spo11-cre)1Rsw/PecoJ), *Gdf9-Cre* (C57BL/6-Tg (Gdf9-icre)5092Coo/J), and *Zp3-Cre* (C57BL/6-Tg(Zp3-cre)93Knw/J)—which resulted in male progeny heterozygous for the *Plk1 del* allele and hemizygous for the germ cell–specific Cre transgene. These mice were bred to female homozygous *Plk1 flox* mice to derive *Plk1* cKO (*Plk1 flox/del*, *Cre*) and control (*Plk1 +/flox*) genotypes.

PCR genotyping

Primers used are described in Supplemental Table S1. PCR conditions: 90°C for 2 min; 30 cycles of 90°C for 20 s, 58°C for annealing, 72°C for 1 min.

Oocyte harvesting and culture

Neonatal mice were harvested 1–2 d postpartum. Ovaries were dissected using methods previously described (Hwang *et al.*, 2018a).

Adult female mice were injected intraperitoneally with 5 IU of equine chorionic gonadotropin (Sigma) to stimulate ovarian follicle development. GV-staged oocytes were harvested from ovaries 44–48 h later. For metaphase II oocytes, mice were injected with 5 IU of equine chorionic, then injected with 5 IU of human chorionic gonadotropin (Sigma) 48 h later. Metaphase II oocytes were harvested from the ampulla 12 h later. Oocytes were cultured in M2 medium supplemented with 5% fetal bovine serum (FBS; Life Technologies), and 3 mg/ml bovine serum albumin (BSA; Sigma-Aldrich). Oocyte-cumulus cell complexes were exposed to 300 IU/ml hyaluronidase (Sigma) in M2 medium supplemented with 3 mg/ml BSA to denude oocytes of surrounding cumulus cells.

For GVBD to metaphase I analyses, oocytes were harvested into M2 medium supplemented with 5% FBS, 3 mg/ml BSA, and 10 mM milrinone (Sigma-Aldrich). The oocytes were then washed and cultured in M2 medium supplemented with 5% FBS and 3 mg/ml BSA, and visually assessed for GVBD throughout a 6-h incubation. For premetaphase timepoints, oocytes were incubated for less time (0 h for dictyate, 2 h for NEBD, and 4 h for prometaphase). Metaphase-stage oocytes were harvested after a 6-h incubation.

Histology and microscopy

For histological assessment of oocytes, ovaries were fixed with Bouin's fixative, sectioned (5 μm thick), and stained with hematoxylin and eosin. Follicle stages were determined by visual assessment, as reported previously (Hwang *et al.*, 2017).

Oocyte chromatin spreads and whole-oocyte mounts for immunofluorescence microscopy analyses were performed using techniques previously described (Hwang *et al.*, 2018a). Primary antibodies used and dilutions are listed in Supplemental Table S2. Secondary antibodies against mouse, rabbit, and human IgG and conjugated

to Alexa 488, 568, or 633 (Life Technologies) were used at 1:500 dilution. Preparations were then mounted with Vectashield + DAPI medium (Vector Laboratories) or Clearmount (Invitrogen).

Images were captured using a Zeiss Cell Observer Z1 linked to an ORCA-Flash 4.0 CMOS camera (Hamamatsu) and analyzed with the Zeiss ZEN 2012 blue edition image software. Photoshop (Adobe) was used to prepare figure images. Images shown are representative of defects and were chosen to demonstrate the observed phenotypes.

Meiotic substages of oocytes were determined visually using either SYCP3, alpha-tubulin, or DNA morphology. For quantification, metaphase-stage oocytes were identified by having condensed chromatin or bipolar alpha-tubulin localization. Quantification of MTOC and LISD components only included oocytes with at least one of those two characteristics.

Spindle dimensions were visualized with alpha-tubulin antibodies and measured using ImageJ (National Institutes of Health). Spindle length was defined as the distance from one spindle pole to the other. Spindle width was measured across the widest part of the spindle.

Graph preparation and statistical analysis was performed using GraphPad Prism (GraphPad Software). Two-tailed Mann-Whitney tests were performed to determine *P* values. The number of samples used for each quantification is included in the corresponding figure legend.

ACKNOWLEDGMENTS

We thank Steve Murray for helping coordinate obtaining the *Plk1* cKO mouse line, Karen Schindler and Andrew Holland for antibodies, and Stephen Wellard and Grace Hwang for technical help.

REFERENCES

Abe S, Nagasaka K, Hirayama Y, Kozuka-Hata H, Oyama M, Aoyagi Y, Obuse C, Hirota T (2011). The initial phase of chromosome condensation requires Cdk1-mediated phosphorylation of the CAP-D3 subunit of condensin II. Genes Dev 25, 863–874.

Attner MA, Miller MP, Ee L, Elkin SK, Amon A (2013). Polo kinase Cdc5 is a central regulator of meiosis I. Proc Natl Acad Sci USA 110, 14278–14283.

Baumann C, Wang X, Yang L, Viveiros MM (2017). Error-prone meiotic division and subfertility in mice with oocyte-conditional knockdown of pericentrin. J Cell Sci 130, 1251–1262.

Burkhardt S, Borsos M, Szydlowska A, Godwin J, Williams SA, Cohen PE, Hirota T, Saitou M, Tachibana-Konwalski K (2016). Chromosome cohesion established by REC8-cohesin in fetal oocytes is maintained without detectable turnover in oocytes arrested for months in mice. Curr Biol 26, 678–685.

Challa K, Fajish VG, Shinohara M, Klein F, Gasser SM, Shinohara A (2019). Meiosis-specific prophase-like pathway controls cleavage-independent release of cohesin by Wapl phosphorylation. PLoS Genet 15, e1007851.

Champion L, Linder MI, Kutay U (2017). Cellular reorganization during mitotic entry. Trends Cell Biol 27, 26–41.

Clift D, Schuh M (2015). A three-step MTOC fragmentation mechanism facilitates bipolar spindle assembly in mouse oocytes. Nat Commun 6, 7217.

de Castro IJ, Gil RS, Ligammari L, Di Giacinto ML, Vagnarelli P (2018). CDK1 and PLK1 coordinate the disassembly and reassembly of the nuclear envelope in vertebrate mitosis. Oncotarget 9, 7763–7773.

Fu W, Chen H, Wang G, Luo J, Deng Z, Xin G, Xu N, Guo X, Lei J, Jiang Q, *et al*. (2013). Self-assembly and sorting of acentrosomal microtubules by TACC3 facilitate kinetochore capture during the mitotic spindle assembly. Proc Natl Acad Sci USA 110, 15295–15300.

Gray S, Cohen PE (2016). Control of meiotic crossovers: from double-strand break formation to designation. Annu Rev Genet 50, 175–210.

Haarhuis JHI, Elbatsh AMO, Rowland BD (2014). Cohesin and its regulation: on the logic of X-shaped chromosomes. Dev Cell 31, 7–18.

Hwang GH, Hopkins JL, Jordan PW (2018a). Chromatin spread preparations for the analysis of mouse oocyte progression from prophase to metaphase II. J Vis Exp 132, e56736.

Hwang G, Sun F, O'Brien M, Eppig JJ, Handel MA, Jordan PW (2017). SMC5/6 is required for the formation of segregation-competent bivalent chromosomes during meiosis I in mouse oocytes. Development 144, 1648–1660.

Hwang G, Verver DE, Handel MA, Hamer G, Jordan PW (2018b). Depletion of SMC5/6 sensitizes male germ cells to DNA damage. Mol Biol Cell mbcE18070459.

Jackman M, Lindon C, Nigg EA, Pines J (2003). Active cyclin B1-Cdk1 first appears on centrosomes in prophase. Nat Cell Biol 5, 143–148.

Jessberger R (2012). Age-related aneuploidy through cohesion exhaustion. EMBO Rep 13, 539–546.

Kim JH, Shim J, Ji M, Jung Y, Bong SM, Jang Y, Yoon E, Lee S, Kim KG, Kim YH, *et al*. (2014). The condensin component NCAPG2 regulates microtubule-kinetochore attachment through recruitment of Polo-like kinase 1 to kinetochores. Nat Commun 5, 4588.

Lan Z-J, Xu X, Cooney AJ (2004). Differential oocyte-specific expression of Cre recombinase activity in GDF-9-iCre, Zp3cre, and Msx2Cre transgenic mice. Biol Reprod 71, 1469–1474.

Lee BH, Amon A (2003). Role of Polo-like kinase CDC5 in programming meiosis I chromosome segregation. Science 300, 482–486.

Lee I-W, Jo Y-J, Jung S-M, Wang H-Y, Kim N-H, Namgoong S (2017). Distinct roles of Cep192 and Cep152 in acentriolar MTOCs and spindle formation during mouse oocyte maturation. FASEB J 32, 625–638.

Lee K, Rhee K (2011). PLK1 phosphorylation of pericentrin initiates centrosome maturation at the onset of mitosis. J Cell Biol 195, 1093–1101.

Liao Y, Lin D, Cui P, Abbasi B, Chen C, Zhang Z, Zhang Y, Dong Y, Rui R, Ju S (2018). Polo-like kinase 1 inhibition results in misaligned chromosomes and aberrant spindles in porcine oocytes during the first meiotic division. Reprod Domest Anim 53, 256–265.

Linder MI, Köhler M, Boersema P, Weberruss M, Wandke C, Marino J, Ashiono C, Picotti P, Antonin W, Kutay U (2017). Mitotic disassembly of nuclear pore complexes involves CDK1- and PLK1-mediated phosphorylation of key interconnecting nucleoporins. Dev Cell 43, 141–156.e7.

Lyndaker AM, Lim PX, Mleczko JM, Diggins CE, Holloway JK, Holmes RJ, Kan R, Schlafer DH, Freire R, Cohen PE, *et al*. (2013). Conditional inactivation of the DNA damage response gene Hus1 in mouse testis reveals separable roles for components of the RAD9-RAD1-HUS1 complex in meiotic chromosome maintenance. PLoS Genet 9, e1003320.

Ma W, Baumann C, Viveiros MM (2010). NEDD1 is crucial for meiotic spindle stability and accurate chromosome segregation in mammalian oocytes. Dev Biol 339, 439–450.

MacLennan M, Crichton JH, Playfoot CJ, Adams IR (2015). Oocyte development, meiosis and aneuploidy. Semin Cell Dev Biol 45, 68–76.

Mardin BR, Agircan FG, Lange C, Schiebel E (2011). Plk1 controls the Nek2A-PP1γ antagonism in centrosome disjunction. Curr Biol 21, 1145–1151.

Martino L, Morchoisne-Bolhy S, Cheerambathur DK, Van Hove L, Dumont J, Joly N, Desai A, Doye V, Pintard L (2017). Channel nucleoporins recruit PLK-1 to nuclear pore complexes to direct nuclear envelope breakdown in *C. elegans*. Dev Cell 43, 157–171.e7.

Mishra RK, Chakraborty P, Arnaoutov A, Fontoura BMA, Dasso M (2010). The Nup107-160 complex and γ-TuRC regulate microtubule polymerization at kinetochores. Nat Cell Biol 12, 164–169.

Mogessie B, Scheffler K, Schuh M (2018). Assembly and positioning of the oocyte meiotic spindle. Annu Rev Cell Dev Biol 34, 381–403.

Nagaoka SI, Hassold TJ, Hunt PA (2012). Human aneuploidy: mechanisms and new insights into an age-old problem. Nat Rev Genet 13, 493–504.

Namgoong S, Kim N-H (2018). Meiotic spindle formation in mammalian oocytes: implications for human infertility. Biol Reprod 98, 153–161.

Pahlavan G, Polanski Z, Kalab P, Golsteyn R, Nigg EA, Maro B (2000). Characterization of polo-like kinase 1 during meiotic maturation of the mouse oocyte. Dev Biol 220, 392–400.

Prosser SL, Pelletier L (2017). Mitotic spindle assembly in animal cells: a fine balancing act. Nat Rev Mol Cell Biol 18, 187–201.

Schatten H, Sun Q-Y (2015). Centrosome and microtubule functions and dysfunctions in meiosis: implications for age-related infertility and developmental disorders. Reprod Fertil Dev 27, 934–943.

So C, Seres KB, Steyer AM, Mönnich E, Clift D, Pejkovska A, Möbius W, Schuh M (2019). A liquid-like spindle domain promotes acentrosomal spindle assembly in mammalian oocytes. Science 364 eaat9557.

Solc P, Kitajima TS, Yoshida S, Brzakova A, Kaido M, Baran V, Mayer A, Samalova P, Motlik J, Ellenberg J (2015). Multiple requirements of PLK1 during mouse oocyte maturation. PLoS One 10, e0116783.

Sun S-C, Liu H-L, Sun Q-Y (2012). Survivin regulates Plk1 localization to kinetochore in mouse oocyte meiosis. Biochem Biophys Res Commun 421, 797–800.

Torosantucci L, De Luca M, Guarguaglini G, Lavia P, Degrassi F (2008). Localized RanGTP accumulation promotes microtubule nucleation at kinetochores in somatic mammalian cells. Mol Biol Cell 19, 1873–1882.

Wang H, Choe MH, Lee I-W, Namgoong S, Kim J-S, Kim N-H, Oh JS (2017). CIP2A acts as a scaffold for CEP192-mediated microtubule organizing center assembly by recruiting Plk1 and aurora A during meiotic maturation. Development 144, 3829–3839.
Webster A, Schuh M (2017). Mechanisms of aneuploidy in human eggs. Trends Cell Biol 27, 55–68.
Xiong B, Sun S-C, Lin S-L, Li M, Xu B-Z, OuYang Y-C, Hou Y, Chen D-Y, Sun Q-Y (2008). Involvement of Polo-like kinase 1 in MEK1/2-regulated spindle formation during mouse oocyte meiosis. Cell Cycle 7, 1804–1809.
Zhang X, Chen Q, Feng J, Hou J, Yang F, Liu J, Jiang Q, Zhang C (2009). Sequential phosphorylation of Nedd1 by Cdk1 and Plk1 is required for targeting of the γTuRC to the centrosome. J Cell Sci 122, 2240–2251.